Taylor & Francis
Taylor & Francis Group

Cell Communication & Adhesion

ISSN: 1541-9061 (Print) 1543-5180 (Online) Journal homepage: informahealthcare.com/journals/icac20

Fabrication of nanofiber coated with l-arginine via electrospinning technique: a novel nanomatrix to counter oxidative stress under crosstalk of co-cultured fibroblasts and satellite cells

Sivakumar Allur Subramaniyan, Sunirmal Sheet, Saravanakumar Balasubramaniam, Swami Vetha Berwin Singh, Dileep Reddy Rampa, Sureshkumar Shanmugam, Da Rae Kang, Ho Sung Choe & Kwan Seob Shim

To cite this article: Sivakumar Allur Subramaniyan, Sunirmal Sheet, Saravanakumar Balasubramaniam, Swami Vetha Berwin Singh, Dileep Reddy Rampa, Sureshkumar Shanmugam, Da Rae Kang, Ho Sung Choe & Kwan Seob Shim (2018) Fabrication of nanofiber coated with l-arginine via electrospinning technique: a novel nanomatrix to counter oxidative stress under crosstalk of co-cultured fibroblasts and satellite cells, Cell Communication & Adhesion, 24:1, 19-32, DOI: 10.1080/15419061.2018.1493107

To link to this article: https://doi.org/10.1080/15419061.2018.1493107

Published online: 05 Sep 2018.

CELL COMMUNICATION & ADHESION
2018, VOL. 24, NO. 1, 19–32
https://doi.org/10.1080/15419061.2018.1493107

Taylor & Francis
Taylor & Francis Group

RESEARCH ARTICLE

OPEN ACCESS Check for updates

Fabrication of nanofiber coated with L-arginine via electrospinning technique: a novel nanomatrix to counter oxidative stress under crosstalk of co-cultured fibroblasts and satellite cells

Sivakumar Allur Subramaniyan[a], Sunirmal Sheet[b], Saravanakumar Balasubramaniam[c], Swami Vetha Berwin Singh[d], Dileep Reddy Rampa[e], Sureshkumar Shanmugam[f], Da Rae Kang[a], Ho Sung Choe[a] and Kwan Seob Shim[a]

[a]Department of Animal Biotechnology, College of Agriculture and Life Sciences, Chonbuk National University, Jeonju-si, Republic of Korea; [b]Department of Wood Science and Technology, College of Agriculture and Life Sciences, Chonbuk National University, Jeonju-si, Republic of Korea; [c]School of Chemistry and Environment, South China Normal University, Guangshou, China; [d]Molecular Imaging and Therapeutic Medicine Research Center, Cyclotron Research Center, Research Institute of Clinical Medicine, Biomedical Research Institute, Chonbuk National University, Medical School and Hospital, Jeonju-si, Republic of Korea; [e]Department of BIN convergence Technology, College of Engineering, Chonbuk National University, Jeonju, Republic of Korea; [f]Department of Animal Science and BK21 PLUS program, Jeonju-si, Republic of Korea

ABSTRACT

The objective of this study was to synthesize and characterize novel polyurethane (PU)-nanofiber coated with L-arginine by electrospinning technique. This study determined whether L-arginine conjugated with PU-nanofiber could stimulate cell proliferation and prevent H_2O_2-induced cell death in satellite cells co-cultured with fibroblasts isolated from Hanwoo (Korean native cattle). Our results showed that L-arginine conjugated with PU nanofiber could reduce cytotoxicity of co-cultured satellite cells. Protein expression levels of bcl-2 were significantly upregulated whereas those of caspase-3 and caspase-7 were significantly downregulated in co-culture of satellite cells compared to those of monoculture cells after treatment with PU-nanofiber coated with L-arginine and which confirmed by Confocal microscope. These results suggest that co-culture of satellite cells with fibroblasts might be able to counter oxidative stress through translocation/penetration of antioxidant, collagen, and molecules secreted to satellite cells. Therefore, this nanofiber might be useful as a wound dressing in animals to counter oxidative stresses.

ARTICLE HISTORY
Received 4 March 2018
Revised 4 June 2018
Accepted 19 June 2018

KEYWORDS
Co-culture; cell–cell communication; nanofiber; oxidative stress and apoptosis

Introduction

In tissue engineering, natural or synthetic materials can be used as scaffolds for cells to proliferate in a conducive growth environment. Nanofiber scaffolds has been implanted in the human body for rebuilding the integrity of normal human tissue (Borjigin et al. 2012). It has been shown that electro-spun nanofibers can support growth and proliferation of a wide variety of cell types, including mouse fibroblasts, human bone marrow-derived mesenchymal stem cells, human satellite cells, rodent myoblast cells, embryonic stem cells, neural stem cells, and neurite extension.

In particular, biodegradable scaffolds fabricated from synthetic polymers such as polyurethane (PU) are excellent choices for cell growth and tissue engineering due to the ease of electrospinning and their biocompatibility (Bhardwaj and Kundu 2010). Considering unique properties of olive oil and silver nanoparticles (Ag NPs), for the first time, herein we report the fabrication of olive oil/polyurethane composite nanofibrous packaging mats decorated with L-arginine nanoparticles by electrospinning. Electrospinning is one of the simple and most successful methods to fabricate fibers from a broad range of materials such as polymers, ceramics and metals (Amna et al. 2015). Nano-and micro-fibers can be developed by electrospinning technique to create materials for applications in the biomedical field, such as wound dressings (Andreu et al. 2015) and water purification to remove pathogenic microorganisms (Cooper et al. 2013). The general goal of nanofiber design is to provide an ideal structure that can replace the natural extracellular

CONTACT Kwan Seob Shim ksshim@jbnu.ac.kr; Ho Sung Choe hschoe55@hanmail.net Department of Animal Biotechnology, Chonbuk National University, Jeonju-si 54896, Republic of Korea
This article has been republished with minor changes. These changes do not impact the academic content of the article.

matrix until host cells can grow and synthesize new natural cellular matrix. Due to huge surface area and microporous structure of electrospun nanofiber mats, they could quickly start signaling pathways and attract fibroblasts to the dermal layer which can excrete important extracellular matrix components such as collagen and several cytokines (e.g. growth factors and angiogenic factors) to repair damaged tissue (Prabaharan et al. 2011).

Increased production of reactive oxygen species (ROS) leads to increased level of oxidative stress which plays a role in the etiology of superficial punctate keratopathy and impairs corneal wound healing (Bryan et al. 2012). However, when ROS cellular overproduction overwhelms the intrinsic antioxidant capacity, oxidative stress will occur, causing damage to biomolecules of normal cells and tissues due to activation of apoptotic proteins and cellular necrosis (Atilano et al. 2005). ROS encompass a variety of free radicals, including the superoxide anion (O^{2-}), hydroxyl radical ($OH^{\bullet}$), singlet oxygen ($^1O_2$), and hydrogen peroxide (H_2O_2) (Subramaniyan et al. 2016). H_2O_2 is a molecule can readily penetrate cell membranes and generate the most reactive form of oxygen and $OH^{\bullet}$ radical, could inducing oxidative stress in *in vitro* models (Schmidley 1990).

Antioxidant supplementation to the medium may reduce or inhibit ROS generation, thus suppressing ROS damage and various antioxidants such as L-arginine have been used as ROS scavengers in various species (Greene et al. 2013). L-arginine is considered a conditionally essential amino acid for healthy mature mammals and young developing mammals for tissue growth (Flynn et al. 2002). In this study, PU was used as a foundation polymer and blended with L-arginine to achieve desirable properties such as better cell viability, cell attachment, and proliferation with enhanced antioxidant ability by preventing ROS production.

Satellite cells in postnatal skeletal muscle are mononucleated myogenic precursors located beneath the basal lamina of myofibers (Bischoff 1986). It can regulate postnatal muscle growth and muscle repair in the agricultural community (Dodson et al. 2015). Fibroblasts as predominant cells found in connective tissues are primary sources of extracellular matrix components such as collagen. Likewise, fibroblasts provide tensile and compressive strength to organs and tissues also ability to synthesis of new collagen is essential for health. It is mainly present in skin, bones, tendons, cartilages, and teeth (Siwik et al. 2001). However, molecular mechanisms involved in the interaction between satellite cells and fibroblasts is unclear. To the best of our knowledge, there has been no report on the effect of L-ascorbic acid conjugated with PU nanofiber on satellite cells co-cultured with fibroblast cells. Therefore, the objective of this study was to determine the effect of L-arginine conjugated with PU nanofiber on growth, migration, and apoptosis pathways in H_2O_2-induced satellite cells co-cultured with fibroblast cells compared to monoculture satellite cells. The present study will provide an understanding of the molecular mechanisms involved in the interaction between satellite cells and fibroblast cells under oxidative stress, an important biological event in animals.

Materials and methods

Materials

Polyurethane (PU, $Mw = 110{,}000$) was purchased from CardioTech International (Japan). L-arginine was purchased from Sigma Aldrich (St. Louis, MO, USA). iScript TM cDNA Synthesis Kit (170-8891) and SsoFast EvaGreen Supermix (172-5202) were procured from Bio-Rad (Bio-Rad Laboratories, Inc., Hercules, CA, USA). Primers were obtained from Genotech (Daejeon, South Korea). Dulbecco's modified Eagle's medium (DMEM) and fetal bovine serum were purchased from Gibco® Life Technologies (Grand Island, NY, USA). All laboratory wares were purchased from Falcon Labware (Becton Dickinson, Franklin Lakes, NJ, USA).

Synthesis of PU-nanofiber conjugated with L-arginine meshes

Polyurethane, 10-wt % was prepared by dissolving in solvent of DMF: THF (1:1) for overnight to make polymer solution. 2-wt % of L-arginine powder was added to the polymer (PU) solution. A high voltage power supply (CPS-60 K02V1, Chungpa EMT, South Korea) of 22 kV with a syringe micro-tip was used to electrospin nanofibers. A ground iron drum covered by polyethylene sheet served as counter electrode. In this study, we used the conventional electrospinning setup where the syringe was kept inclined to flow the spinning solution. The tip-to-collector distance was kept at 15 cm. Polymer solution was fed to the 5 ml syringe with a plastic micro-tip. A horizontal electrospinning set up was used. The addition of L-arginine significantly decreased solution viscosity. Inclination of the syringe was adjusted to prevent dropping of the solution. It also prevented beads formation in the electrospun mat. Addition of L-arginine did not affect solution conductivity or the electrospinning process. Finally, PU-(L-arginine) drug nanofiber mats were vacuum dried in an oven at 30 °C for 24 h to remove residual solvent. These samples were used for further characterizations.

Isolation of satellite cells from Hanwoo *cattle*

Satellite cells were isolated from 24-month-old Korean native cattle (*Hanwoo*) of *emitendinosus* (SM) muscle (500 g) following published method (Dodson et al. 1987). All experiments involving the use of animals were approved by our Institutional Animal Care and Use Committee. Isolation of intramuscular connective tissue fibroblasts from *Hanwoo* Cattle.

The entire work involving the use of animals was approved by the Institutional Animal Care and Use Committee of Chonbuk National University (CBNU 2015-048 revised in 2015). SM muscles were excised from *Hanwoo* cattle (20–30 months old) immediately after slaughter at a commercial abattoir located in Jeonju Province (South Korea) following the method of Subramaniyan and Hwang (2017).

Co-culture of satellite cells and fibroblast cells

Satellite cells and fibroblast cells were incubated at a density of 6000 cells/cm^2 and grown in DMEM containing 10% FBS and 1% penicillin/streptomycin at 37 °C with 5% CO_2. These cells were then co-cultured using trans-well inserts with a 0.4-μm porous membrane to separate satellite cells and fibroblast cells. Each cell type was grown independently on the trans-well plate. Following cell differentiation, inserts containing adipocytes were transferred to separate fibroblast plates while inserts containing fibroblasts were transferred to adipocyte plates. Following co-culture for 24 and 48 h, lower well cells were treated with H_2O_2 for 4 h and then harvested for further analysis.

Experimental groups

Group 1: (MC)-satellite cells (monoculture); Group 2: (MC + H_2O_2)-satellite cells (monoculture) + H_2O_2; Group 3: (MC + C-NF + H_2O_2)-satellite cells (monoculture) treated with conjugated nanofiber + H_2O_2; Group 4: (CC)-satellite cells (co-culture); Group 5: (CC + H_2O_2) satellite cells (co-culture) + H_2O_2; Group 6: (CC + C–NF + H_2O_2)-satellite cells (co-culture) treated with conjugated nanofiber + H_2O_2. Concentration of H_2O_2 used in this study was at 40 μM. Treatment time was 4 h.

Antiradical activity of conjugated nanofibers against DPPH$^\bullet$ and ABTS$^{\bullet+}$

Radical scavenging activity of nanofiber conjugated with L-arginine was carried out using published method by da Silva Uebel et al. (2016). Briefly, 5, 10, 20, and 40 mg of dried conjugated nanofibers were dipped into 5 ml of DMSO solution in a test-tube and then kept in an ultrasonic bath (UIL-Ultrasonic Co. Ltd., South Korea) for 10 min for dispersion of mixed amino acids. Next, 1 ml of prepared conjugated nanofibers solution was added into the radical solution (0.2 mM of DPPH$^\bullet$ in methanol) and the mixture was kept in the dark for 40 min at 20 °C. After incubation, the absorbance was measured at 517 nm using an UV–visible spectrophotometer with methanol as reference. In this method, ascorbic acid was used as the standard. ABTS$^{\bullet+}$ radical inhibition activity was measured by modified method reported by Sivakumar et al. (2017). Briefly, ABTS$^{\bullet+}$ was dissolved in water at a concentration of 7 mM. The stock solution was mixed with 2.45 mM potassium persulfate (final concentration). The mixture was then reacted for 12 h in the dark and then diluted with ethanol to obtain an absorbance of 0.7 at 734 nm. Nanofibers (1 ml of prepared conjugated nanofibers solution) were then mixed with the ABTS solution and the absorbance of the mixture was monitored at 734 nm after 15 min of incubation.

Mitochondrial activity tests by trypan blue staining

Cytotoxicity and cell viability of nanofiber were measured by 2% trypan blue staining using published method of Subramaniyan et al. (2016). The number of viable cells was estimated in each group by counting in a Neubauer chamber.

AO/EtBr dual staining to detect apoptosis

AO/EtBr staining was performed to detect condensed chromatin of dead apoptotic cells (Sivakumar et al. 2017). Apoptotic cells will uptake EtBr and emit red/orange fluorescence under 550 nm. Acridine orange is a DNA-selective and membrane-permeable fluorescent cationic dye that freely enters normal cell nuclei and emits green fluorescence under 525 nm. Stained cells were viewed under a fluorescence microscope LSM510META (Carl Zeiss, Jena, Germany). During apoptosis, DNA becomes condensed and fragmented. The number of apoptotic cells was counted as a function of the total number of cells present in the field. In each sample, a minimum of 400 cells were counted. The percentage of cells having condensed or fragmented nuclei among total cells was then calculated as a function of the total number of cells present in the field.

Determination of apoptosis and necrosis

FITC/PI Annexin V Apoptosis Detection Kit (BioLegend, Cat # 640914, San Diego, CA, USA) was used to detect

apoptosis and necrosis rates of Ag NP- and Au NP-treated HT-1080 cells according to the manufacturer's instructions. After incubation with Ag NPs and Au NPs for 48 h, HT-1080 cells were harvested, washed with PBS, suspended in Annexin V binding buffer, and incubated with FITC-labeled AnnexinVand PI for 15 min at room temperature in the dark. Samples were then immediately analyzed by flow cytometry (BD, Franklin Lakes, NJ, USA).

Attenuation of ROS generation

Reactive oxygen species levels in experimental groups were estimated by dichloro–dihydro–fluorescein diacetate (DCFH-DA) assay (Subramaniyan et al. 2018). Briefly, experimental cells were incubated with 1 μL of DCFH-DA (13 mM) for 30 min after treatment with compounds. These cells were then washed twice with PBS and processed for estimation of intracellular ROS levels using a spectrofluorophotometer ($\lambda Ex/\lambda Em = 490$ nm/520 nm). Results are expressed as arbitrary units (a.u.) of fluorescence intensity (FI) by spectrofluorometer. Fluorescence microscopic images were taken using a blue filter (450–490 nm) under a fluorescence microscope.

Single-cell gel electrophoresis (comet assay)

DNA damage was estimated by alkaline single-cell gel electrophoresis (comet assay) according to the method of Singh et al. (1988). Briefly, a layer of 1% NMPA was prepared on microscope slides. All experiment cells were mixed with 200 μl of 0.5% LMPA. Slides were immersed in cold lysis solution at pH 10 (2.5M NaCl, 10 mM Na_2 EDTA, 10 mM Tris pH 10, 1% Triton X-100, 10%DMSO) and kept at 4 °C for 60 min. To allow denaturation of DNA, slides were placed in alkaline electrophoresis buffer at pH 13 and left for 25 min. These slides were then neutralized with 0.4M Tris (pH 7.5) for 5 min and stained with 20 mg/ml of EtBr. For visualization of DNA damage, observations were made using a 409 objective of an epifluorescent microscope equipped with an excitation filter of 510–560 nm and a barrier filter of 590 nm. DNA damage was quantified by tail length. Twenty-five images were randomly selected from each sample and were examined at 40× magnification in a fluorescence microscope connected to a personal computer-based image analysis system. Images were captured with a digital camera with networking capability and analyzed by image analysis software. The relative amount of DNA appearing in the tail of the comet (percent tail DNA).

Mode of interaction of conjugated nanoparticles with satellite cell membranes

For scanning electron microscopy (SEM), cells were grown on coverslips in six-well plate at 37 °C with 5% CO_2 atmosphere. In order to examine cell attachment manner on composite nanofibers, chemical fixation was carried out for each sample. After various treatments, cells were fixed with 2% paraformaldehyde and 2% (vol/vol) glutaraldehyde at room temperature, washed with washing solution (0.05M sodium cacodylate buffer, pH 7.2), and postfixed with 1% (vol/vol) osmium tetroxide in 0.05M sodium cacodylate buffer (pH 7.2). These coverslips were then washed with washing solution followed by en block staining (1% (vol/vol) uranyl acetate). Dehydration was performed in a graded series of alcohol afterward. Coverslips were then air-dried at room temperature, mounted on aluminum sample stubs, and gold-coated by sputtering. Finally, these coverslips were observed by FE-SEM.

Immunocytochemistry of caspase-3 activation

Experiment cells were seeded on a glass coverslip in trans-well plate (3×10^5 cells per well plates) for 24 h. These cells were then treated with nanofibers for 24 h following previous method of Subramaniyan and Hwang (2017). After the incubation time, cells were fixed with 3% paraformaldehyde in PPS for 10 min and then washed twice with PBS. Cells were permeabilized in 0.1% Triton X-100 in PBS for 10 min and then washed twice with PBS. Blocking was performed in 3% BSA in PBS for 30 min. Cells were then incubated with cas-3 primary antibody (1:500 dilutions) overnight at 4 °C. After that, cells were washed three times with PBS and incubated with secondary fluorescein isothiocyanate (FITC) conjugated antibody at room temperature for 1 h. The coverslip was mounted with fluorescent mounting medium (Dako, Trappes, France) and visualized under a fluorescence microscope (Carl Zeiss, Jena, Germany). All the values were expressed as means of six ($n = 6$) determinations. Fluorescence intensity was analyzed and quantified with Image-Pro Plus Scientific Software, version 5.1 (Media Cybernetics)

Apoptotic protein expression by Western blot

Total protein was isolated from experiment cells using RIPA buffer to check protein expression levels of Bcl-2, cas-3 and cas-7. Protein concentration was determined using Bio-Rad protein assay kit (Bio-Rad). Protein samples (25 μg) were solubilized in *Laemmli* buffer and separated by 6% acrylamide with 4% acrylamide stacking gels. They were then transferred onto Hybond-P PVDF

membrane (GE Healthcare, Amersham, UK) for 60 min at 200 mA. After blocking with 5% skimmed milk powder in 0.5M Tris-buffered saline, pH 7.4 with 0.05% Tween-20 (TBST) at room temperature for 2 h, immunoblot was incubated with Bcl-2, cas-3, and cas-7 primary antibody (1:5000 dilution) overnight at 4 °C. After three times washing with TBST, these membranes were incubated with an HRP-conjugated secondary antibody (1:2000 dilutions) at room temperature for 60 min. After washing thrice with TBST (10 min each wash), protein bands were visualized using enhanced chemiluminescence assay kit (Western Bright TM ECL, CA 94025, USA), scanned, and quantified with Image J Software. The relative density ratio of band was normalized to that of GAPDH.

Quantitative real-time polymerase chain reaction (qRT-PCR)

Total cellular RNA was extracted from all experimental groups using TriZol reagent. The purify of prepared RNA was checked with a μDrop plate (Thermo Fisher Scientific, USA). Then cDNA was synthesized with iScript™ cDNA synthesis kit (Bio-Rad) using 2 μg of total RNA. Reverse transcription polymerase chain reaction assays were performed on a CFX96™ real-time PCR detection system (Bio-Rad). The cDNA was then used as template to amplify each gene. PCR reaction was carried out according to the manufacturer's instructions (Bio-Rad). Real-time PCR was performed using a cDNA equivalent from each sample's total RNA at amount of 10 ng with primers (Table 1) specific for caspase-3, caspase-7, and β-actin as a housekeeping gene. Real-time PCR results were used to calculate cycle threshold difference ΔCt ($Ct_{\text{gene of interest}} - Ct_{\text{reporter gene}}$). Relative gene expression levels were then obtained using $\Delta\Delta Ct$ method ($\Delta Ct_{\text{sample}} - \Delta Ct_{\text{calibrator}}$). The conversion between $\Delta\Delta Ct$ and relative gene expression levels was as follows: fold induction $=2^{-\Delta\Delta Ct}$ (Livak and Schmittgen 2001).

Statistical analysis

Data for biochemical analyses are expressed as mean ± SD ($n = 6$). Statistical evaluation was carried out by one-way analysis of variance (ANOVA) followed by Duncan's multiple range test (DMRT). Student's *t*-test was used to determine statistical differences between PU-nanofiber coated with L-arginine and PU-nanofiber

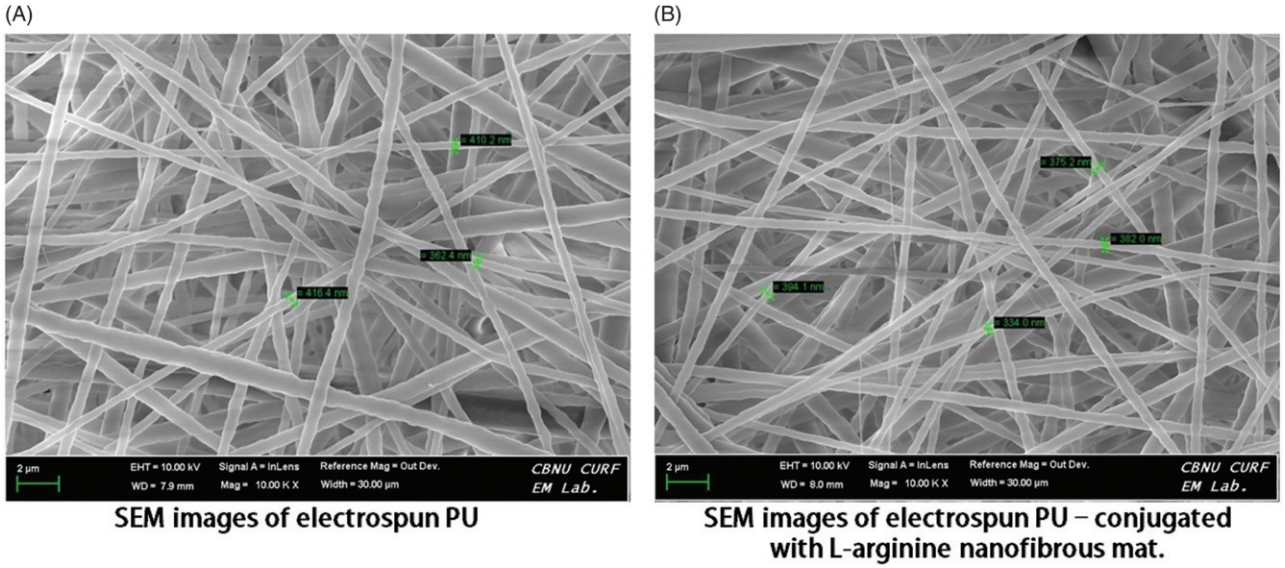

Figure 1. Scanning electron microscopy images of electrospun (A) PU and (B) PU-drug nanofibrous mats.

Table 1. List of primers for qRT-PCR.

Gene	Primer sequences (5′-3′)	Product size
CAS-3	Forward 5′-GCAAACCTCAGGGAAACATT-3′ Reverse 5′-TTGCATGAAAAGCAGAATCG-3′	562
CAS-7	Forward 5′- AAGGCCATATTGTGGAGCAG-3′ Reverse 5′-GGCAAGCCTGAATGAAGAAG-3′	546
β-actin	Forward 5′-CACCCTCAAGATTGTCAGC-3′ Reverse 5′-TAAGTCCCTCCACGATGC-3′	520

not coated with L-arginine. Statistical significance was considered at $p < 0.01$.

Results

Morphological structure studies

Scanning electron microscopy images of electrospun PU and PU-L-arginine (drug) loaded composite nanofibers are shown in Figure 1, respectively. These as-spun nanofibers exhibited smooth surface with uniform diameters along their lengths. As shown in Figure 1(A), no drug crystals were detected on the surface by electron microscopy. Figure 1(B) showed that L-arginine was loaded inside these nanofibers, demonstrating good compatibility of drug–polymer–solvent.

Antiradical activity

L-Arginine attenuated oxidative stress due to the presence of higher antioxidant activity in PU nanofiber. Among concentrations of 5, 10, 20, and 40 mg, higher radical scavenging activity was obtained from 40 mg of nanoparticles in both ABTS and DPPH assays (Figure 2(A and B)).

Mitochondrial activity tests by trypan blue staining

In vitro cell viability is a crucial method to evaluate biocompatibility of fibrous mats. Therefore, co-culture and monoculture of satellite cells on different mats under normal and oxidative stress conditions were prepared. As shown in Figure 2(C), there was significant proliferation of

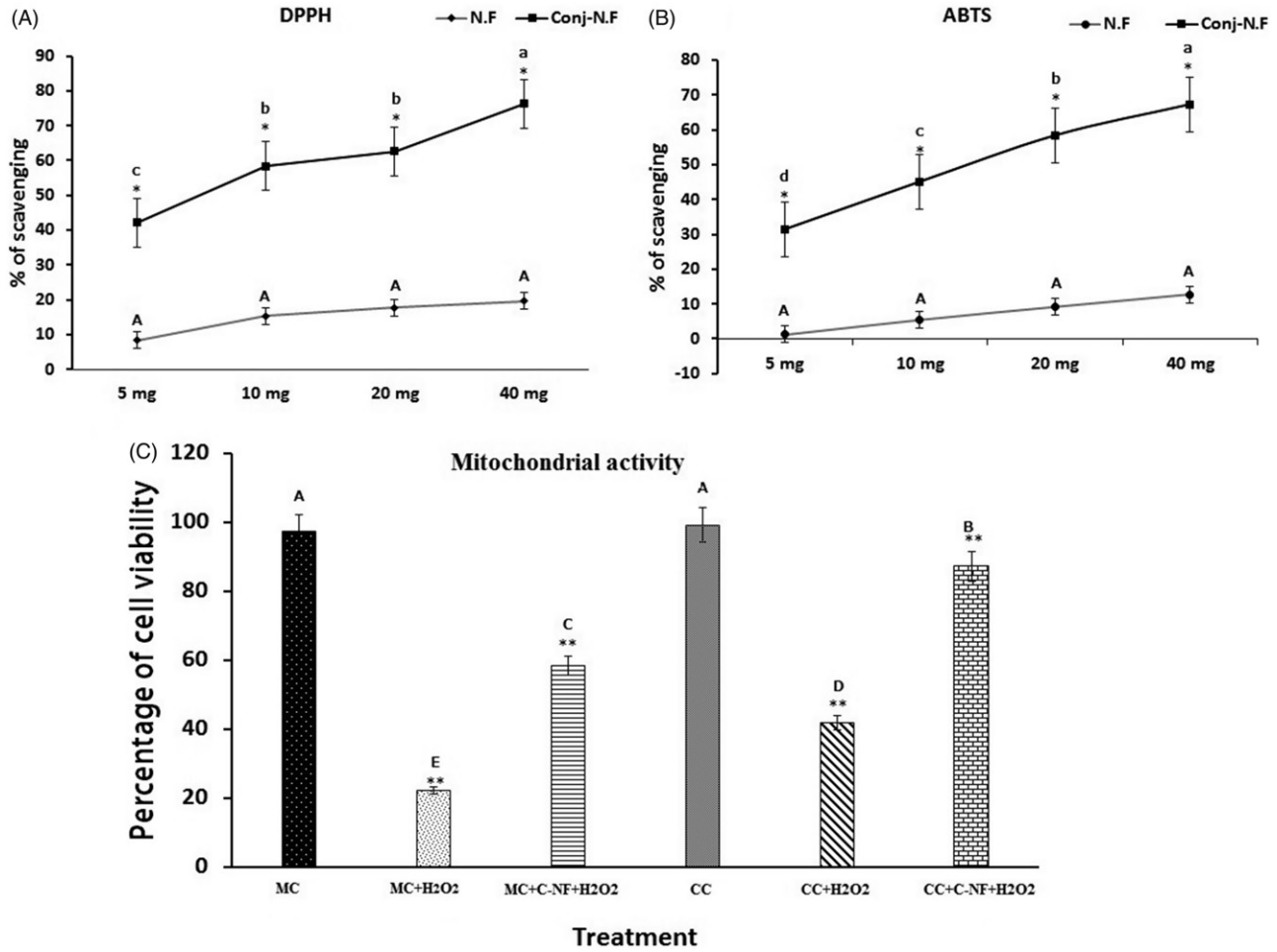

Figure 2. (A) DPPH• radical-scavenging activity of PU-nanofiber coated with L-arginine (5, 10, 20, and 40 mg) and PU-nanofiber non-coated with L-arginine (5, 10, 20, and 40 mg). Absorbance values were converted to scavenging effects (percent). (B) $ABTS^{+}$ radical-scavenging activity of PU-nanofiber coated with L-arginine (5, 10, 20, and 40 mg) and PU-nanofiber non-coated with L-arginine (5, 10, 20, and 40 mg). Absorbance values were converted to scavenging effects (percent). (C) Cell proliferation was detected by trypan blue staining. (MC)-satellite cells (monoculture); $(MC + H_2O_2)$ satellite cells (monoculture)$+H_2O_2$; $(MC + C–NF + H_2O_2)$-satellite cells (monoculture) treated with conjugated nanofiber $+ H_2O_2$; (CC)-satellite cells (co-culture); $(CC + H_2O_2)$-satellite cells (co-culture) $+ H_2O_2$; $(CC + C–NF + H_2O_2)$-satellite cells (co-culture) treated with conjugated nanofiber $+ H_2O_2$. Values are presented as mean ± SD from six determinations. Large characters indicate significant differences among PU-nanofiber coated with L-arginine groups at $p < 0.01$; **significant compared to the control group at $p < 0.01$.

cells in all groups. PU-L-arginine composite nanofibrous scaffolds supported more viable growth of co-cultured satellite cells compared to PU-nanofibrous scaffolds under monoculture. Cell viability was significantly decreased up to 22.14% in co-cultured satellite cells whereas it was increased up to 41.46% in H_2O_2-induced co-cultured satellite cells. Cell growths of H_2O_2-induced monoculture and co-cultured satellite cells treated with conjugated nanoparticles were significantly increased. In the presence of conjugated nanoparticles, cell viability of co-cultured satellite cells induced by H_2O_2 was significantly increased compared to that of monoculture of satellite cells induced by H_2O_2.

AO/EtBr dual staining to detect apoptosis

Acridine orange/ethidium bromide (Ao/EtBr) were used to detect the apoptotic morphological apoptotic and necrotic cells. Viable cells emit light green fluorescence, early apoptotic having bright green fluorescence, late apoptotic having orange fluorescence and red colored fluorescence uptake nonviable cells. Results are displayed in Figure 3(A and B). H_2O_2 treated cells showed condensed nuclei, membrane blebbing, and apoptotic bodies seen in red. Upon exposure to the nanomatrix conjugated with or without L-arginine, toxicity, apoptosis, and nuclear contraction were decreased while survival rate of H_2O_2 induced cells was increased. Figure 3(B) is a bar blot showing the % of apoptosis in the experimental group.

Determination of apoptosis and necrosis

Figure 3(C) shows representative Annexin V/PI results of satellite cells treated with conjugated nanofiber. Cells treated with conjugated nanofibers exhibited reduced apoptosis (56.42% and 37.47% in MC + C–NF + H_2O_2 and CC + C–NF + H_2O_2 groups, respectively). There were no apoptotic cells detected in control cells (monoculture or co-culture of satellite cells). Figure 3(D) is a bar blot showing the % of apoptosis and necrosis in the experimental group.

Attenuation of ROS generation

Satellite cells were treated with H_2O_2 to generate ROS under monoculture and co-cultured conditions. Microscopic fluorescence images of DCF fluorescence in different treatment groups are shown in Figure 4(A and B). Compared to the control group, H_2O_2 treatment groups showed increased DCF fluorescence whereas fluorescence was decreased in both mono-cultured and co-cultured satellite cells. Fluorescence of H_2O_2-induced cells after treatment with PU-nanofiber conjugated with L-arginine was more decreased compared to that in other treatment groups. Figure 6(A) shows spectrofluorometric readings of DCF fluorescence in experimental groups. Upon treatment with PU-nanofiber conjugated with L-arginine, ROS levels were decreased in H_2O_2 induced satellite cells under mono- and co-cultured conditions. Decreased ROS generation in H_2O_2 treatment cells showed an additive effect in the presence of PU-nanofiber conjugated with L-arginine. A significant decrease in ROS levels (4.6-fold) was found in PU-nanofiber conjugated with L-arginine treated group whereas 1.7- and 1.4-fold increases in H_2O_2 induced satellite cells were found under mono- and co-cultured conditions, respectively. Figure 4(B) is a bar blot showing the fluorescence intensity of ROS level in the experimental group.

Single-cell gel electrophoresis (comet assay)

Figure 6 illustrates the occurrence of DNA damage in terms of formation of DNA in the tail and variation in tail length in L-arginine meshes treated cells. There were significant differences between monoculture and co-culture of satellite cells shows in Figure 6(C and D). No such changes were observed in untreated monoculture and co-culture of satellite cells. H_2O_2 resulted in significant increase in the percentage of formation of DNA tail length, clearly substantiating the occurrence of DNA damage. Figure 4(D) is a bar blot showing the % of tail length of DNA in the experimental group.

Mode of interaction of conjugated nanofiber with satellite cell membranes

Morphological changes of treated cells were also observed by SEM analysis. Results are depicted in Figure 5(A). It was evident that PU-L-arginine conjugated nanofiber could induce more cell growth of co-cultured satellite cells under oxidative stress condition (induced by H_2O_2) than that of monoculture cells under the same condition. Under oxidative condition, cell morphology was changed compared to control cells.

Immunocytochemistry of caspase-3 activation

To examine changes of collagen type I in satellite cells and fibroblast cells adipocytes, we performed immunofluorescent staining for collagen type I. H_2O_2-induced monoculture of satellite cells showed decreased fluorescence of collagen type I expression. The fluorescence of collagen type I expression in H_2O_2-

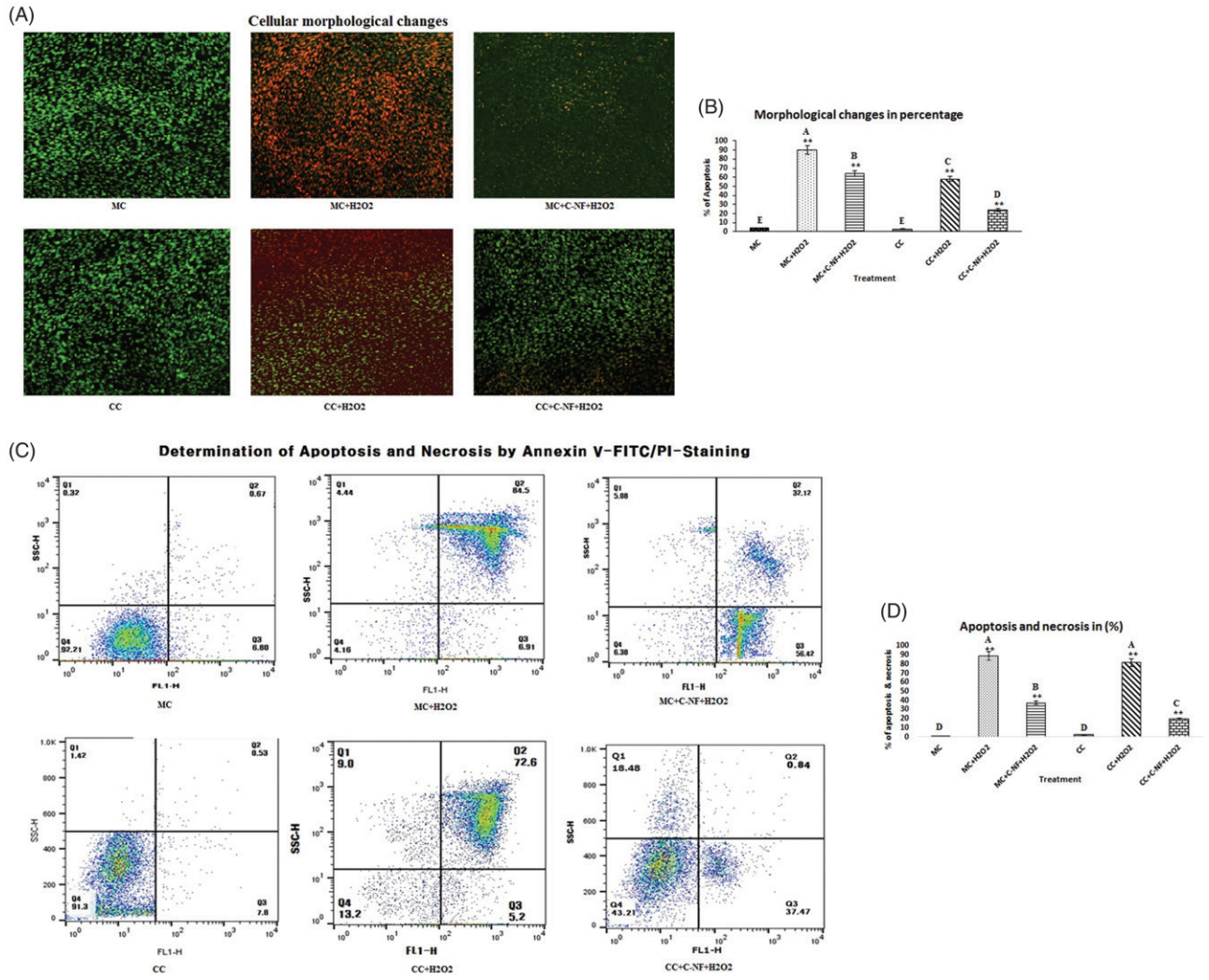

Figure 3. (A) Cellular morphological changes observed under a fluorescence microscope using OA/EtBr staining (×20). (MC)-satellite cells (monoculture); (MC + H_2O_2) satellite cells (monoculture)+H_2O_2; (MC + C-NF + H_2O_2)-satellite cells (monoculture) treated with conjugated nanofiber + H_2O_2; (CC)-satellite cells (co-culture); (CC + H_2O_2)-satellite cells (co-culture) + H_2O_2; (CC + C-NF + H_2O_2)-satellite cells (co-culture) treated with conjugated nanofiber + H_2O_2. (B) Bar graph represents the quantitative comparison among the groups. (C) H_2O_2-induced apoptosis and necrosis rate in mono- and co-culture satellite cells in the presence of PU-nanofiber coated with L-arginine or PU-nanofiber non-coated with L-arginine. (C) Bar graph represents the quantitative comparison among the groups.

induced co-cultured satellite cells with fibroblast cells was increased compared to that in monoculture of satellite cells under oxidative stress condition. Results of distribution of collagen type I in satellite cells and fibroblast cells are present in Figure 5(B and C). Contact of fibroblast cells with satellite cells by translocation of collagen might have prevented cell rupture under oxidative stress. Moreover, H_2O_2-induced cell death occurred more in the monoculture of fibroblast cells and 3T3–L1 cells compared to that in the co-culture. H_2O_2 can induce cell death in adipocytes by inhibiting antioxidant enzymes such as catalase. Based on our study, it was evident that cell viability was significantly increased in H_2O_2-induced co-culture of satellite cells compared to that in monoculture of satellite cells. Figure 5(C) is a bar blot showing the fluorescence intensity of cas-3 in the experimental group.

Apoptotic protein expression by Western blot

Results of western blotting revealed that expression levels of apoptotic-related proteins such as cas-3 and cas-7 were significantly decreased in H_2O_2- treated satellite cells (co-culture or monoculture) in the presence of conjugated nanofiber compared to those in H_2O_2- treated cells in the absence of conjugated nanofiber (Figure 6(A)). Bcl-expression was significantly downregulated in both monoculture and co-culture of H_2O_2 treated satellite cells, but upregulated after treatment with PU-nanofiber conjugated with L-arginine. Figure 6(B–D) are a bar blot

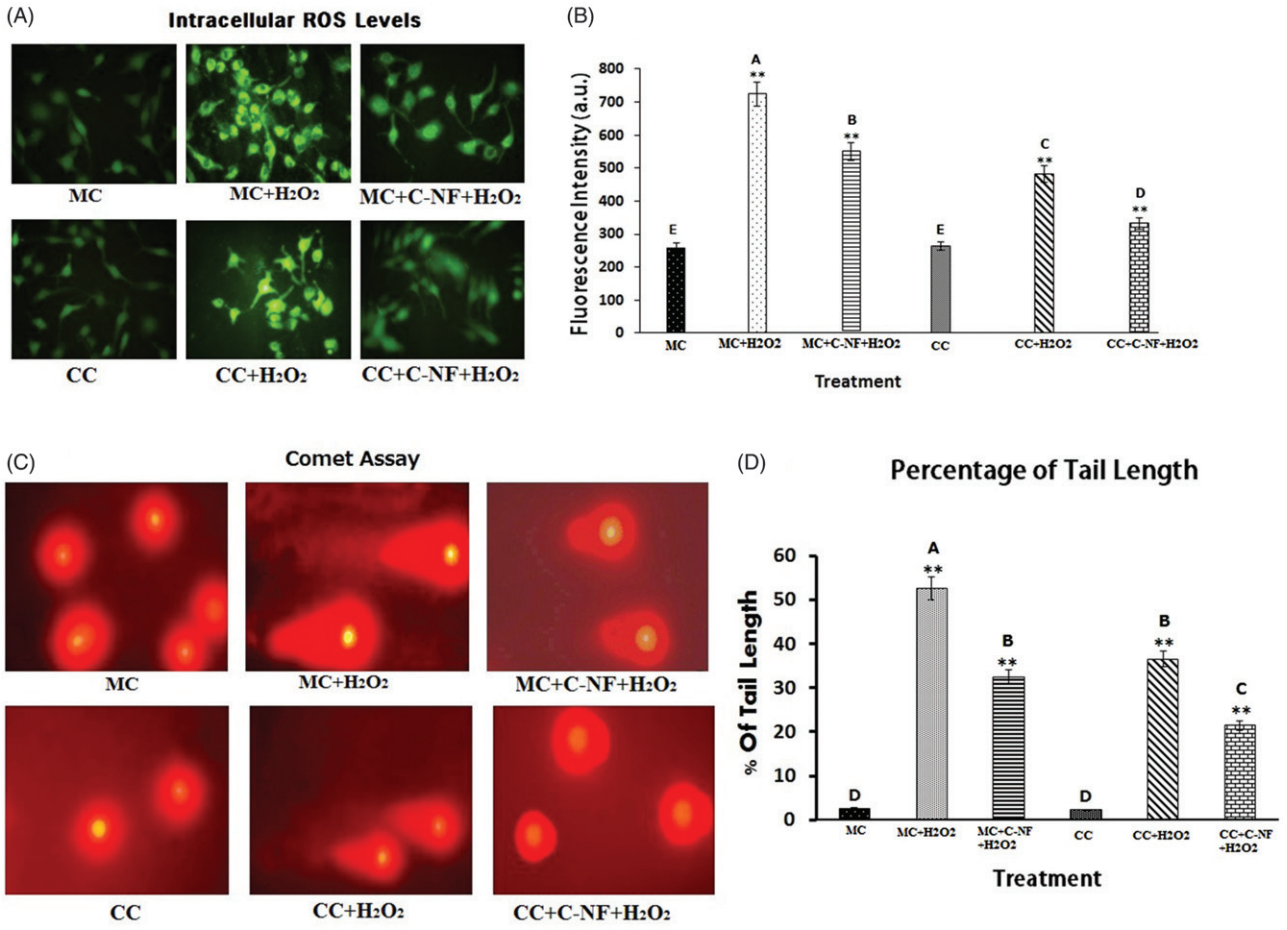

Figure 4. (A) ROS generation in H_2O_2-induced satellite cells under mono- and co-culture conditions. (C) Microscopic images showing damage and repair of DNA damage by comet assay. (MC)-satellite cells (monoculture); $(MC + H_2O_2)$ satellite cells (monoculture)$+H_2O_2$; $(MC + C\text{-}NF + H_2O_2)$-satellite cells (monoculture) treated with conjugated nanofiber $+ H_2O_2$; (CC)-satellite cells (co-culture); $(CC + H_2O_2)$-satellite cells (co-culture) $+ H_2O_2$; $(CC + C\text{-}NF + H_2O_2)$-satellite cells (co-culture) treated with conjugated nanofiber $+ H_2O_2$. (B and C) Bar graph represents the quantitative comparison among the groups. Values are given as mean $\pm$ SD of six determinations. Large characters indicate significant differences among PU-nanofiber coated with L-arginine groups at $p < 0.01$; **significant as compared to the control group at $p < 0.01$.

showing the expression of Bcl-2, cas-3, and cas-7 in the experimental group. These results are expressed as density ratio to β-actin after normalization.

Quantitative real-time polymerase chain reaction (qRT-PCR)

Figure 7 shows mRNA abundance of caspase-3 and caspase-7 in monoculture and co-culture of fibroblast and satellite cells under oxidative stress conditions with and without treatment of PU-nanofiber conjugated with L-arginine. Expression levels of caspase-3 and caspase-7 were significantly downregulated in the presence of PU-nanofiber conjugated with L-arginine group in both monoculture and co-culture of satellite cells. These genes were significantly down-regulated in co-culture than those in monoculture of satellite cells. On the other hand, monoculture of H_2O_2-induced fibroblast cells showed significant upregulation in their expression levels compared to the control. H_2O_2-induced oxidative stress in monoculture cells caused increased activation of NF-κB and TNF-α. However, levels of NF-κB and TNF-α were reduced under co-culture conditions. This might be due to penetration of antioxidant enzymes from 3T3–L1 to fibroblast or fibroblast to 3T3–L1 cells. The production of antioxidant enzymes from adipose tissue can protect cells from apoptosis through downregulating caspases.

Discussion

These results of our scavenging radical activity were consistent with a previous report showing that PCL nanofiber conjugated with quercetin had the highest

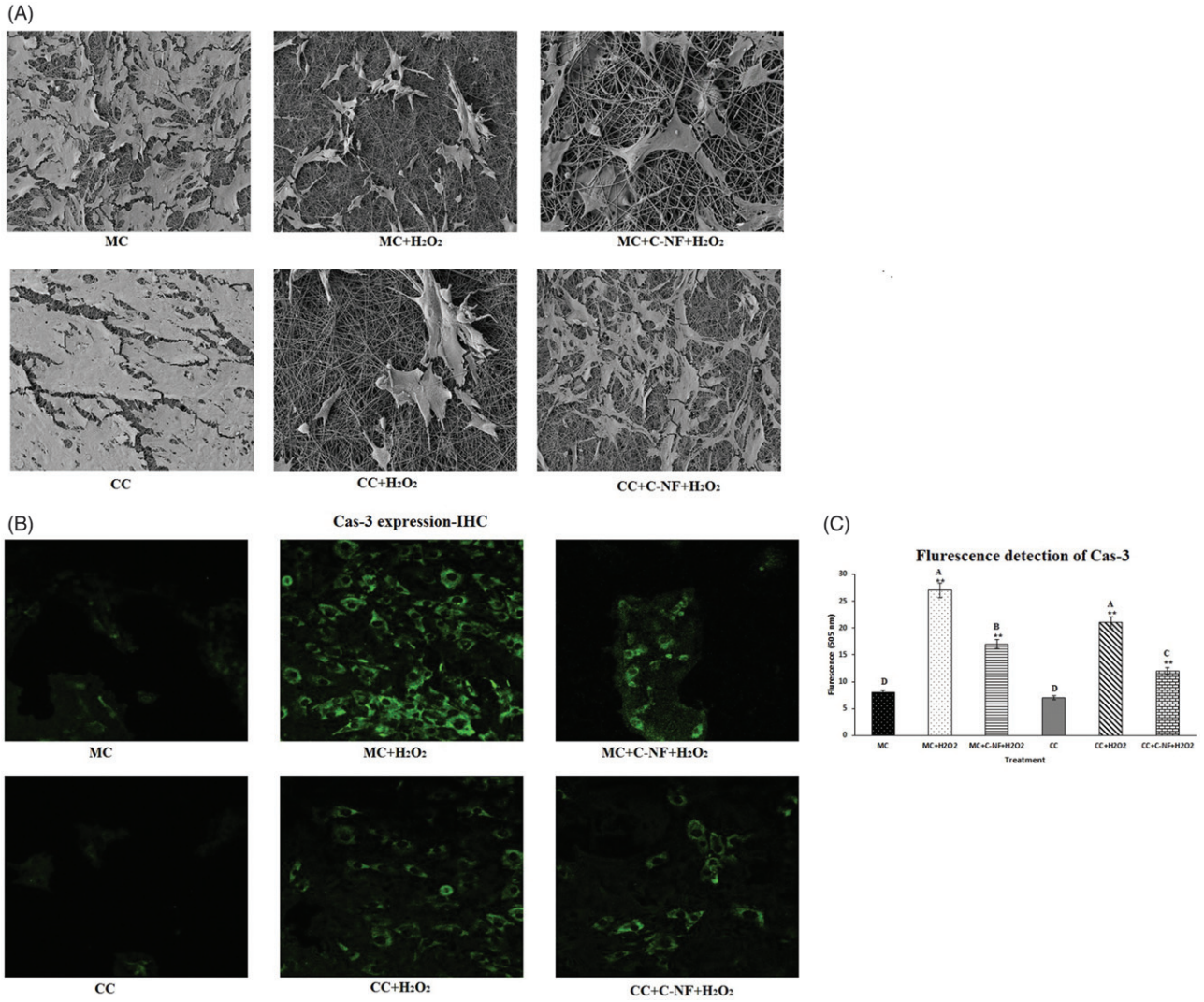

Figure 5. (A) 3D images of morphological changes in treated cells observed by SEM. (B) Immunocytochemistry of cas-3 expression. (MC)-satellite cells (monoculture); (MC + H_2O_2) satellite cells (monoculture)+H_2O_2; (MC + C-NF + H_2O_2)-satellite cells (monoculture) treated with conjugated nanofiber + H_2O_2; (CC)-satellite cells (co-culture); (CC + H_2O_2)-satellite cells (co-culture) + H_2O_2; (CC + C-NF + H_2O_2)-satellite cells (co-culture) treated with conjugated nanofiber + H_2O_2. (C) Image-Pro Plus software was used to quantitate fluorescence intensities. Bar graph represents the quantitative comparison among the groups. All the values were expressed as means of six ($n = 6$) determinations.

antioxidant activity in DPPH and ABTS assays (da Silva Uebel et al. 2016). Inhibition between 25% and 50% is considered as median range while DPPH inhibition of more than 75% is considered as having the best antioxidant activity. The quercetin coated with poly(ε-caprolactone) scaffold and polymeric nanoparticles respectively exhibited free radical scavenging activity against DPPH and could prevent the tissue damage and accelerating the healing process (da Silva Uebel et al. 2016). Hence, PU nanofiber containing L-Arginine released rapidly which may reduce adverse effects found in damaged tissues by removing products of radicals and reduce oxidative stress.

Previous study showing that co-cultured satellite cells with fibroblasts could increase cell growth when compared to monoculture of satellite cells (Subramaniyan et al. 2016). Similarly, PU-dextran nanofibrous scaffolds have increased cell growth of fibroblasts compared to PU scaffolds (Unnithan et al. 2012). In our study, PU-L-Arginine nanofibrous scaffold was suitable for growth of H_2O_2 induced co-cultured satellite cells than monoculture. Treatment with ferulic acid encapsulated nanofibers reduced the cytotoxicity against hepatocellular carcinoma (HepG2) (Vashisth et al. 2015). Moreover, niclosamide-AgNPs composite nanofibers showed more orange-red color fluorescence compared to control MCF-7 and A549 cells (Vashisth et al. 2015). However, for the first time, we found that PU nanofibrous scaffold conjugated with L-arginine could reduce the orange-red color and increase the green color appearance in co-cultured satellite cells

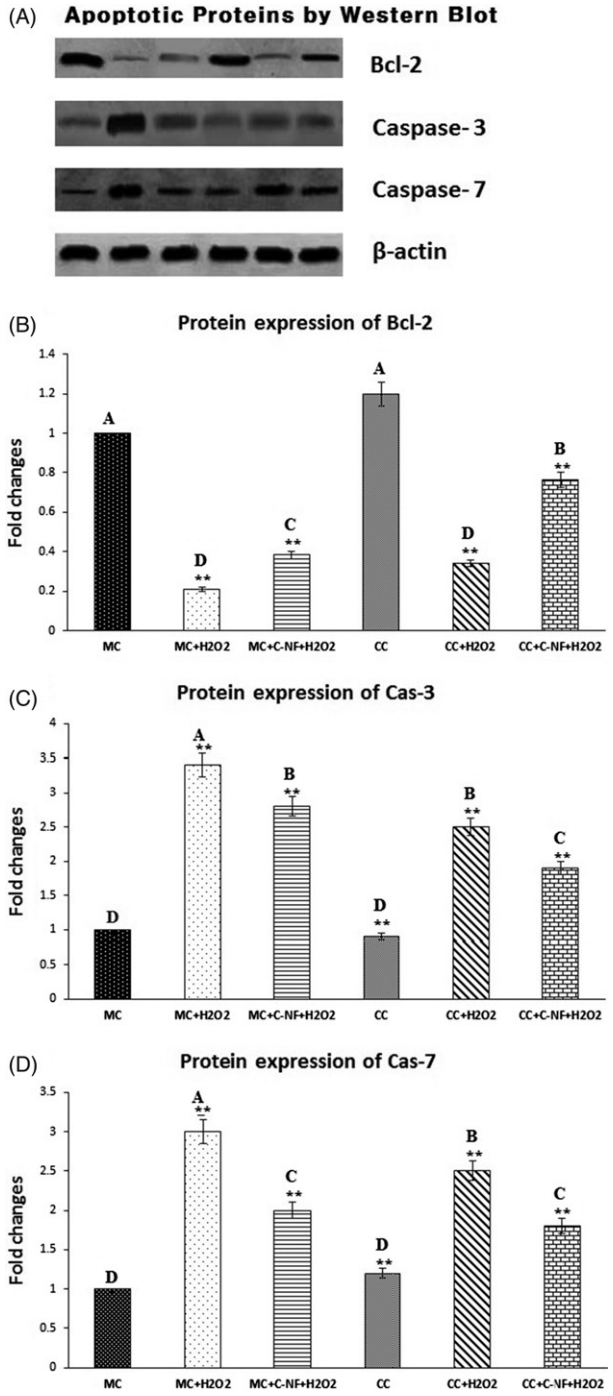

Figure 6. (A) Western blot showed that expression levels of bcl-2, cas-3, and cas-7. (MC)-satellite cells (monoculture); (MC + H_2O_2) satellite cells (monoculture)+H_2O_2; (MC + C-NF + H_2O_2)-satellite cells (monoculture) treated with conjugated nanofiber + H_2O_2; (CC)-satellite cells (co-culture); (CC + H_2O_2)-satellite cells (co-culture) + H_2O_2; (CC + C-NF + H_2O_2)-satellite cells (co-culture) treated with conjugated nanofiber + H_2O_2. (B) Bar graph represents the quantitative comparison among the groups. Data are expressed as a relative intensity ratio compared to β-actin. Values are presented as mean ± SD from six determinations. Large characters indicate significant differences among PU-nanofiber coated with L-arginine groups at $p < 0.01$; **significant as compared to the control group at $p < 0.01$. Data are expressed as the ratio of the relative intensity with β-actin.

than monoculture under oxidative stress condition. Therefore, encapsulated L-arginine released from the PU-nanofiber can reduce apoptosis and promote cell growth by preventing oxidative stress. Apoptosis/necrosis is a physiological mode of programmed cell death that plays an important role in a variety of cellular events. The apoptotic process involves characteristic cell change, cell shrinkage, nuclear fragmentation and chromatin condensation. Therefore, flow cytometry was performed to quantitatively determine the percentage of cells undergoing cellular apoptosis or necrosis in our current study. Based on flow cytometry analysis, it has been found that cytotoxicity of docetaxel-loaded poly-D, L-lactide nanofibers could induce apoptosis in 4T1 cells (Ding et al. 2016). Our present results point out that PU-nanofiber conjugated with L-arginine prevent the apoptosis and necrosis of satellite cells under oxidative stress.

Cerium oxide NPs-loaded nanofibers reduced levels of fluorescence, indicating that they could scavenge ROS levels produced by oxidative stress (H_2O_2). Moreover, less cell viability was found in monoculture of satellite cells, indicating buildup of oxidative damage due to their inadequate ROS scavenging nature compared to co-culture (Rather et al. 2018). Fibroblasts are the most common cells for collagen synthesis and SOD production during oxidative stress (Subramaniyan et al. 2016). The same mechanism might have occurred in the treatment with L-arginine during co-culture results attenuate oxidative stress through the suppression of ROS production. Thus, decreased ROS formation can attenuate inhibition of cell proliferation which can be increased by L-arginine supplementation (Tripathi & Pandey, 2013). In our study, increase of cell viability by L-arginine released from PU-nanofiber might be due to its anti-oxidative and ROS scavenging activity, possessed antioxidant activity which may cause cell protection and cytoprotection against oxidative damage. Therefore, PU-nanofiber conjugated with L-arginine meshes can be explored as wound dressing materials due to their antioxidant potential. Single-cell gel electrophoresis (comet assay) was carried out to determine apoptotic changes in our experimental group. Induction of cellulose nanofibers in lymphocytes and fibroblasts results increased in DNA tail length and the DNA strand breaking were measured by comet and DNA fragmentation assay respectively (de Lima et al. 2012). However, findings of the present study were in contrast with the previous work. Our resulted showed that treatment with L-arginine meshes caused a decreases in the number of tail DNA and tail length.

In *in vivo* studies, treatment of L-arginine has accelerated the repair of intestinal mucosa and stimulated cell-proliferation (Raul et al. 1995). Likewise, it has been

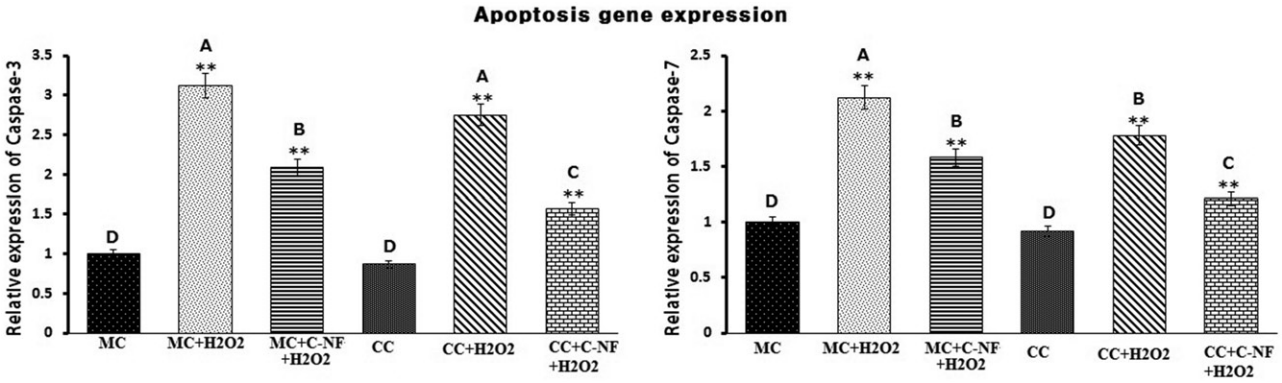

Figure 7. Bar diagram representing RT-PCR results of cas-3 and cas-7. The results depicted are normalized to levels of β-actin and expressed relative to the control. (MC)-satellite cells (monoculture); (MC + H_2O_2) satellite cells (monoculture)+H_2O_2; (MC + C-NF + H_2O_2)-satellite cells (monoculture) treated with conjugated nanofiber + H_2O_2; (CC)-satellite cells (co-culture); (CC + H_2O_2)-satellite cells (co-culture) + H_2O_2; (CC + C-NF + H_2O_2)-satellite cells (co-culture) treated with conjugated nanofiber + H_2O_2. Large characters indicate significant differences among PU-nanofiber coated with L-arginine groups at $p < 0.01$; **significant as compared to the control group at $p < 0.01$.

reported that L-arginine, play a multiple physiological role in the human body also support to cell growth. Cell morphology has changed by oxidative condition could be due to the L-arginine can stimulate cell proliferation to repair damaged cells and tissues through NO– and polyamine-mediated mechanisms (Tan et al. 2009). L-Arginine can also improve wound healing and cell proliferation by stimulation of T-cell responses that can escalate the fibroblast responses. Elevation of collagen deposition and wound breaking strength have effective against aging related disease due to its antioxidant activities (Barbul 1988). This same mechanism might have occurred in our current study that during oxidative stress condition, collagen might have penetrated from fibroblast cells to satellite cells to prevent cell death. In addition, it has enhanced cell-penetrating ability to target cells due to their anti-aging and anti-oxidant activity. Moreover, collagen can protect brain cells against amyloid beta protein, the accumulation of which can lead to Alzheimer's disease (Cheng et al. 2009). Our results agreed with a previous study that suggests a cross-talk between these two cell types by molecules secreted into cell media that can influence gene transcription, protein expression, and cell viability.

Release of cytochrome c from mitochondrial intermembrane space can be confirmed by caspase activity, is an intracellular cysteine protease that can be activated during the cascade of events associated with apoptosis marker such as cas-3, cas-7, Bcl-2, and Bax (Muñoz-Pinedo et al. 2006). Brain-derived neurotrophic factor activation was shown to upregulate Bcl-2, downregulate Bax, inhibit caspase-3 activation (Liu et al. 2015). In the current study, expression levels of cas-3 and cas-7 were increased more in monoculture of satellite cells than those in co-cultured satellite cells, suggesting that H_2O_2 induced more increase of apoptosis in satellite cells under monoculture condition than co-culture condition. Our results are consistent with a previous study of Holen et al. (2014) proposed that there might be a cross talk between these two cell types by molecules secreted into the cell media that can influence protein expression and cell viability. Moreover, the molecular mechanism for caspase-independent apoptosis-like cell death regulated by L-arginine involves ROS mediated DNA degradation through depolarization of mitochondrial membrane potential along with cytosolic cytochrome-c release (Mandal et al. 2016). Gene expression levels of cas-3, TNF-α, and NF-κB in H_2O_2-stressed monoculture cells were increased compared to co-culture. Fibroblast and 3T3–L1 cells might share secreted molecules with each other under co-culture condition through the culture medium. Such secreted molecules including SOD, adiponectin, and PPAR-γ can downregulate apoptosis and inflammation through attenuation of caspases, TNF-α, and NF-κB. Adiponectin might be able to penetrate from adipocytes to other neighboring cells to improve cell growth under oxidative stress condition (Subramaniyan et al. 2016). Co-culture of liver cells can elevate or reduce gene transcription compared to monoculture (Holen et al. 2014). However, the role of fibroblast and satellite cells in H_2O_2-induced co-culture after treatment with PU-nanofiber conjugated with L-arginine meshes has not been reported yet. In our current experiment, co-culture of satellite cells might have been protected by collagen synthesis and antioxidant relate molecules released from fibroblast cells as well as L-arginine released from PU-nanofiber thus preventing H_2O_2-induced oxidative stress.

Conclusions

In this study, continuous and uniform nanofibers of PU and a blend of these polymers loaded with L-arginine by electrospinning were successfully obtained. Addition of the drug reduced the size and narrowed the distribution of electrospun nanofiber diameters. This might have contributed to their ability to decrease cell death and apoptosis. The addition of L-arginine into PU increased cell attachment and viability. It also decreased oxidative stress induced by H_2O_2 in co-culture of satellite cells compared to that in monoculture of satellite cells. L-arginine could be released from these composite nanofiber mats and penetrate from one cell to another cell, thus enhancing secreted molecules to prevent cell death caused by free radicals production and oxidative stress. This work provides a basic understanding to design efficient nanofiber-based anti-oxidative materials. The present study concludes that PU-nanofiber conjugated with L-arginine meshes can significantly reduce the oxidative stress via augmentation of antioxidant system in co-cultured satellite cells and fibroblast cells. Additional studies are under way to determine the molecular mechanism and the effect of PU-nanofiber coated with L-arginine on wound healing using an *in vivo* model.

Disclosure statement

No potential conflict of interest was reported by the authors.

Funding

This work was carried out with the support of "Cooperative Research Program for Agriculture Science and Technology Development (Project No. PJ01316702), Republic of Korea.

References

Amna T, Yang J, Ryu K-S, Hwang I. 2015. Electrospun antimicrobial hybrid mats: innovative packaging material for meat and meat-products. *J Food Sci Technol*. 52:4600–4606.

Andreu V, Mendoza G, Arruebo M, Irusta S. 2015. Smart dressings based on nanostructured fibers containing natural origin antimicrobial, anti-inflammatory, and regenerative compounds. *Materials* 8:5154–5193.

Atilano SR, Coskun P, Chwa M, Jordan N, Reddy V, Le K, Wallace DC, Kenney MC. 2005. Accumulation of mitochondrial DNA damage in keratoconus corneas. *Invest Ophthalmol Vis Sci*. 46:1256–1263.

Barbul A. 1988. Role of T-cell-dependent immune system in wound healing. *Prog Clin Biol Res*. 266:161–175.

Bhardwaj N, Kundu SC. 2010. Electrospinning: a fascinating fiber fabrication technique. *Biotechnol Adv*. 28:325–347.

Bischoff R. 1986. Proliferation of muscle satellite cells on intact myofibers in culture. *Dev Biol*. 115:129–139.

Borjigin M, Strouse B, Niamat RA, Bialk P, Eskridge C, Xie J, Kmiec EB. 2012. Proliferation of genetically modified human cells on electrospun nanofiber scaffolds. *Mol Ther Nucl Acids* 1:e59.

Bryan N, Ahswin H, Smart N, Bayon Y, Wohlert S, Hunt JA. 2012. Reactive oxygen species (ROS)–a family of fate deciding molecules pivotal in constructive inflammation and wound healing. *eCM* 24:249.

Cheng JS, Dubal DB, Kim DH, Legleiter J, Cheng IH, Yu G-Q, Tesseur I, Wyss-Coray T, Bonaldo P, Mucke L. 2009. Collagen VI protects neurons against Aβ toxicity. *Nat Neurosci*. 12:119

Cooper A, Oldinski R, Ma H, Bryers JD, Zhang M. 2013. Chitosan-based nanofibrous membranes for antibacterial filter applications. *Carbohydr Polym*. 92:254–259.

da Silva Uebel L, Angelica Schmatz D, Goettems Kuntzler S, Lima Dora C, Luiza Muccillo-Baisch A, Alberto Vieira Costa J, Greque de Morais M. 2016. Quercetin and curcumin in nanofibers of polycaprolactone and poly (hydroxybutyrate-co-hydroxyvalerate): assessment of in vitro antioxidant activity. *J Appl Polym Sci*. 133:43712.

de Lima R, Feitosa LO, Maruyama CR, Barga MA, Yamawaki PC, Vieira IJ, Teixeira EM, Corrêa AC, Mattoso LH, Fraceto LF. 2012. Evaluation of the genotoxicity of cellulose nanofibers. *Int J Nanomed*. 7:3555.

Ding Q, Li Z, Yang Y, Guo G, Luo F, Chen Z, Yang Y, Qian Z, Shi S. 2016. Preparation and therapeutic application of docetaxel-loaded poly(d,l-lactide) nanofibers in preventing breast cancer recurrence. *Drug Deliv*. 23:2677–2685.

Dodson MV, Allen RE, Du M, Bergen WG, Velleman SG, Poulos SP, Fernyhough-Culver M, Wheeler MB, Duckett SK, Young MRI, et al. 2015. Invited review: evolution of meat animal growth research during the past 50 years: Adipose and muscle stem cells. *J Anim Sci*. 93:457–481.

Dodson M, Martin E, Brannon M, Mathison B, McFarland D. 1987. Optimization of bovine satellite cell-derived myotube formation in vitro. *Tissue Cell* 19:159–166.

Flynn N, Meininger C, Haynes T, Wu G. 2002. The metabolic basis of arginine nutrition and pharmacotherapy. *Biomed Pharmacother*. 56:427–438.

Greene JM, Feugang JM, Pfeiffer KE, Stokes JV, Bowers SD, Ryan PL. 2013. L-arginine enhances cell proliferation and reduces apoptosis in human endometrial RL95-2 cells. *Reprod Biol Endocrinol*. 11:15.

Holen E, Espe M, Andersen SM, Taylor R, Aksnes A, Mengesha Z, Araujo P. 2014. A co culture approach show that polyamine turnover is affected during inflammation in Atlantic salmon immune and liver cells and that arginine and LPS exerts opposite effects on p38MAPK signaling. *Fish Shellfish Immunol*. 37:286–298.

Liu B, Zhang YH, Jiang Y, Li LL, Chen Q, He GQ, Tan XD, Li CQ. 2015. Gadd45b is a novel mediator of neuronal apoptosis in ischemic stroke. *Int J Biol Sci*. 11:353–360.

Livak KJ, Schmittgen TD. 2001. Analysis of relative gene expression data using real-time quantitative PCR and the $2-\Delta\Delta CT$ method. *Methods* 25:402–408.

Mandal A, Das S, Roy S, Ghosh AK, Sardar AH, Verma S, Saini S, Singh R, Abhishek K, Kumar A, et al. 2016. Deprivation of L-arginine induces oxidative stress mediated apoptosis in Leishmania donovani promastigotes: contribution of the polyamine pathway. *PLoS Negl Trop Dis*.10:e0004373.

Muñoz-Pinedo C, Guío-Carrión A, Goldstein JC, Fitzgerald P, Newmeyer DD, Green DR. 2006. Different mitochondrial intermembrane space proteins are released during apoptosis in a manner that is coordinately initiated but can vary in duration. *Proc Natl Acad Sci U S A*103:11573–11578.

Prabaharan M, Jayakumar R, Nair S. 2011. Electrospun nanofibrous scaffolds-current status and prospects in drug delivery. Biomedical applications of polymeric nanofibers. Berlin, Heidelberg: Springer; p. 241–62.

Rather HA, Thakore R, Singh R, Jhala D, Singh S, Vasita R. 2018. Antioxidative study of Cerium Oxide nanoparticle functionalised PCL-Gelatin electrospun fibers for wound healing application. *Bioact Mater*. 3:201.

Raul F, Galluser M, Schleiffer R, Gossé F, Hasselmann M, Seiler N. 1995. Beneficial effects of L-arginine on intestinal epithelial restitution after ischemic damage in rats. *Digestion* 56:400–405.

Schmidley J. 1990. Free radicals in central nervous system ischemia. *Stroke* 21:1086–1090.

Singh NP, McCoy MT, Tice RR, Schneider EL. 1988. A simple technique for quantitation of low levels of DNA damage in individual cells. *Exp Cell Res*. 175:184–191.

Sivakumar AS, Krishnaraj C, Sheet S, Rampa DR, Kang DR, Belal SA, Kumar A, Hwang IH, Yun S-I, Lee YS, Shim KS. 2017. Interaction of silver and gold nanoparticles in mammalian cancer: as real topical bullet for wound healing—a comparative study. *In Vitro Celldevbiol-Anim*. 53:632–645.

Siwik DA, Pagano PJ, Colucci WS. 2001. Oxidative stress regulates collagen synthesis and matrix metalloproteinase activity in cardiac fibroblasts. *Am J Physiol Cell Physiol*. 280:C53–C60.

Subramaniyan SA, Hwang I. 2017. Biological differences between Hanwoo longissimus dorsi and semimembranosus muscles in collagen synthesis of fibroblasts. *Korean J Food Sci Anim Resour*. 37:392.

Subramaniyan SA, Kim S, Hwang I. 2016. Cell-cell communication between fibroblast and 3T3-L1 cells under co-culturing in oxidative stress condition induced by H_2O_2. *Appl Biochem Biotechnol*. 180:668–681.

Subramaniyan SA, Sheet S, Vinothkannan M, Yoo DJ, Lee YS, Belal SA, Shim KS. 2018. One-pot facile synthesis of Pt nanoparticles using cultural filtrate of microgravity simulated grown *P. chrysogenum* and their activity on bacteria and cancer cells. *J Nanosci Nanotechnol*.18:3110–3125.

Tan B, Li XG, Kong X, Huang R, Ruan Z, Yao K, Deng Z, Xie M, Shinzato I, Yin Y, Wu G. 2009. Dietary L-arginine supplementation enhances the immune status in early-weaned piglets. *Amino Acids* 37:323–331.

Tripathi P, Pandey S. 2013. L-arginine attenuates oxidative stress condition during cardiomyopathy. *Indian J Biochem Biophys*. 50:99–104.

Unnithan AR, Barakat NA, Pichiah PT, Gnanasekaran G, Nirmala R, Cha Y-S, Jung CH, El-Newehy M, Kim HY. 2012. Wound-dressing materials with antibacterial activity from electrospun polyurethane–dextran nanofiber mats containing ciprofloxacin HCl. *Carbohydrate Polym*. 90:1786–1793.

Vashisth P, Kumar N, Sharma M, Pruthi V. 2015. Biomedical applications of ferulic acid encapsulated electrospun nanofibers. *Biotechnol Rep (Amst)*. 8:36–44.